LHCb note 2004-105

Quality assurance of 100 CMS-OB2 sensors

G. Baumann[1], D. Boeni[1], L. Buchmann[1], A. Büchler[1], N. Chiapolini[1], E. Eisenring[1], N. Franz[1], A. Landwehr[1], F. Lehner[1], C. Lois[1,2], T. Mattle[1], T. Müller[1], S. Nüesch[1]

[1] *Physik-Institut der Universität Zürich, Switzerland*

[2] *Universidade de Santiago de Compostela, Spain*

Abstract

This note gives a description of the sensors that will be employed in the Trigger Tracker station of LHCb, type CMS-OB2, and presents the quality assurance program followed by the Silicon Tracker group in order to ensure their functionality. The results on sensor qualification for a first batch of 100 sensors produced by ST Microelectronics are presented.

1 Introduction

The Trigger Tracker (TT) station [1, 2] is part of the tracking system of the LHCb experiment. The station consists of four planar detection layers that will be entirely covered by silicon micro-strip detectors identical to CMS-OB2 sensors [3, 4]. A total of 896 sensors will be employed in the station, and 1100 sensors (including spares) have to be tested to ensure their functionality and check whether they pass the specified acceptance criteria.

The CMS-OB2 detectors are p-on-n type, single-sided, AC coupled sensors, produced from 6" wafers. The physical dimensions of the sensors are 94.4 mm $\times$ 94.6 mm. The nominal thickness of the n-type substrate is 500 μm. The p^+ strip pitch is 183 μm and the width is 46 μm, which results in a w/p ratio of 0.25. The width of the metal strips is 58 μm (12 μm wider than the implant strips), which gives rise to a more stable operation with respect to high bias voltages.

The CMS-OB2 sensors are manufactured by two companies, ST Microelectronics (STM) and Hamamatsu Photonics (HPK). From the total of

Table 1: Geometry parameters and specifications of OB2-CMS sensors produced by STM.

	CMS-OB2 sensors
Wafer size	6”
Overall width	96374 μm
Overall length	94396 μm
Active area width	93869 μm
Active area length	91571 μm
Nominal thickness	(500 $\pm$ 20) μm
Bulk material	n type
Implant	p^+ type
Crystal orientation	$< 100 >$
Pitch	183 μm
Implant width	46 μm
# of strips	512
Biasing	polysilicon
Read-out coupling	AC

Table 2: CMS acceptance criteria for “Class A” OB2-CMS sensors [4, 5, 6].

	CMS-OB2 sensors
Leakage current at 300 V Leakage current at 450 V	< 5 μA < 10 μA
Breakdown voltage	> 550 V
Depletion voltage	100-300 V
Inter-strip capacitance	< 1.3 pF/cm
Coupling capacitance	> 1.2 pF/cm per μm of impl. strip width
Bias resistors	(1.5 $\pm$ 0.5) MΩ

needed sensors, 100 were produced by STM and the remaining 1000 sensors will be produced by HPK. The sensors are received at CERN, and then are shipped to Zürich for testing.

The outline of this note is the following: the sensor quality assurance program followed by the ST group is presented in Section 2. Results of the visual inspection and metrology tests, leakage current, depletion voltage and coupling capacitance measurements, are described and summarized for the first batch of 100 pre-production sensors produced by STM. In Section 3, the database with the sensor probing information is described. In Section 4, the conclusions from our experience are presented.

2 Sensor quality control and first results from the pre-production

The first batch of 100 pre-production sensors, produced by ST Microelectronics, was received from the CMS Silicon Tracker Collaboration and tested in Zürich in June 2004. In this section, we present the tests done to check the quality of the sensors, and the results from our experience.

2.1 Visual Inspection

A visual inspection on all sensors was done in order to detect macroscopic defects. This is an important test, since large defects are easily detected, and can give rise to instabilities in the electrical behaviour of the sensors or an increase of the leakage currents.

First, the sensors were inspected by eye and using a magnifying glass, checking for damage on the strip side and backplane. Then, the full surface of the sensors was inspected under a microscope on a x-y moving table, taking note of scratches and defects, looking for chipped edges, pad bondability or contamination, as well as for the overall sensor cleanliness. In addition, the serial number on the scratch-pad was checked to coincide with the one on the envelope.

According to these defects, a grading procedure was developed:

- Sensors with almost no defects, without deep scratches or chips, and without pad contamination, were classified as A grade.
- Sensors with some superficial scratches (not deep enough to break strips), or slightly chipped edges, or acid damage in less than four strips, or a lot of dirt and dust, or a combination of these, were classified as B grade.

Table 3: Number of sensors according to the visual inspection grade. Only 49% of the sensors were free of defects.

Grade	# of sensors
A	49
B	35
C	16
D	0

- Sensors with chipped edges, or deep scratches, or acid damage in more than four strips, or damaged pads, were classified as C grade.
- Sensors with long and deep scratches or chips, or extremely dirty, were classified as D grade.

In Table 3, the number of sensors according to the visual grading is shown. Only 49% of the sensors were free of defects and classified as A grade sensors. A and B grade sensors could be used to build silicon modules for use in the experiment.

Some examples of the observed defects, like a chipped edge, bad bonding pads, scratches, and shorts among strips, are shown in Figure 1. A large fraction of the defects found on the sensors were scratches, that can give rise to open strips or shorts between neighbouring strips, and therefore affect the detector performance. In some cases, the scratches were covering a large area on the sensors.

2.2 Leakage currents

The leakage current is the reverse current of the pn-junctions. It gives rise to a background noise and is caused by thermally excited minority carriers generated in the depleted region which, due to the electric field, drift to the electrodes. It depends on various factors, like temperature, humidity and time of operation of the sensor. The leakage current gives a first and simple estimation of the quality of the sensors, and it is a crucial test of the global properties of the sensors.

The current between the backplane and the bias ring was measured as a function of the reverse bias voltage for all sensors, using a Keithley 487 unit (picoamperemeter + voltage source). The bias voltage was increased up to 500 V in steps of 5 V, over a period of 5 minutes. The measurements were

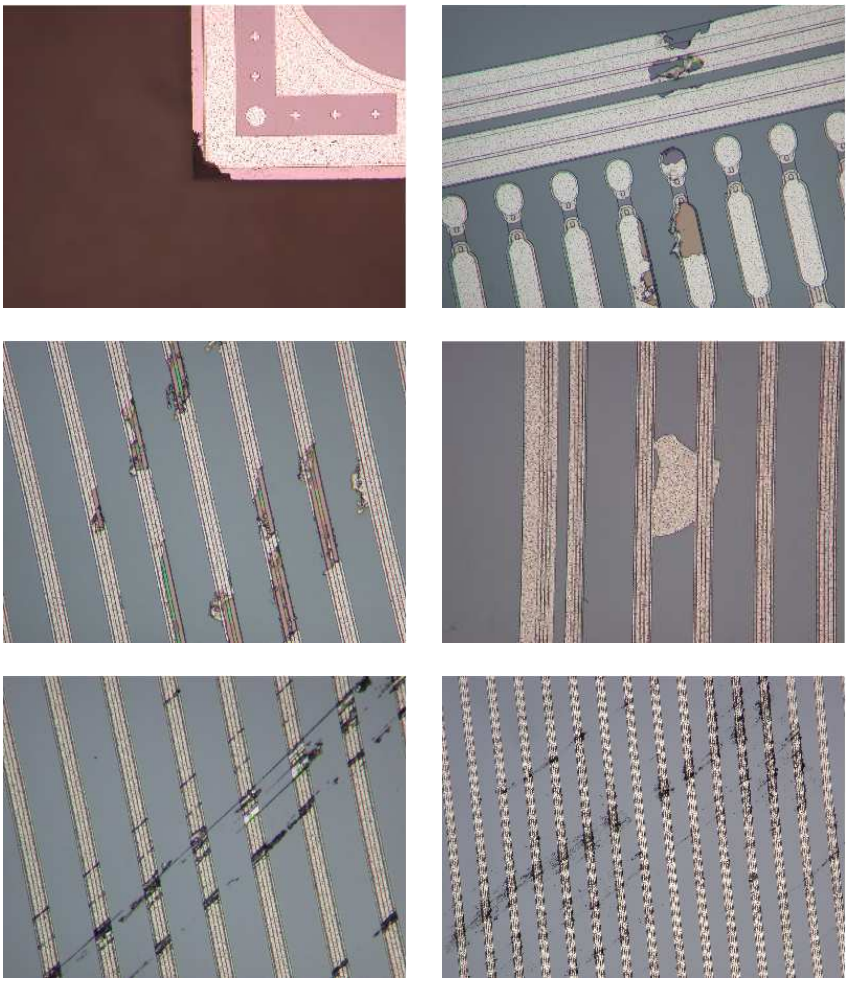

Figure 1: Examples of the defects found on the sensors that were classified as C grade in the visual inspection. On the top, a chipped edge (left) and bad bonding pads (right). In the middle, pictures of open aluminium lines (left) and shorts among strips (right). At the bottom, some examples of scratches are shown.

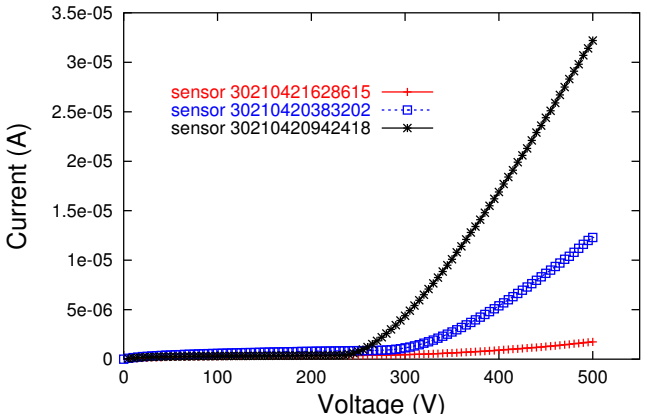

Figure 2: Typical IV curves measured on the sensors. Examples of sensors with low, medium, and high leakage currents have been selected.

performed at room temperature, typically about 20 $^\circ$C, and at a relative humidity below 30%.

In this section, results on leakage currents for the 100 tested sensors are presented. Typical IV curves and the distributions of the currents measured at certain bias voltages are shown. The breakdown voltages are extracted from the IV curves, and their distribution is shown. The current dependence on humidity and on the application of vacuum to the chuck of the probe station are investigated. The stability and repeatability of the curves are also studied.

Typical IV curves are shown in Figure 2. As typical examples, a curve measured for a sensor with low leakage current, one for a sensor with high leakage current, and an intermediate one, are shown. Large differences between sensor currents were found.

Figure 3 shows the distributions of the leakage currents measured at 300 V and 500 V. It can be seen that the currents at 300 V are below 5 μA for most of the sensors, whilst the currents at 500 V spread over a wide range, up to 40 μA. According to CMS specifications, the leakage currents must fulfill three criteria [4]: *i*) maximum value at 300 V less than 5 μA, *ii*) maximum value at 450 V less than 10 μA, *iii*) maximum increase in the range 450-550 V less than 10 μA. About 15% of sensors failed the first criteria, and about 40% of sensors failed either the second or third criteria.

In earlier measurements [7] it had been observed that the leakage currents for sensors produced by STM depended critically on the application of vacuum to hold the sensors to the chuck of the probe station. To investigate this

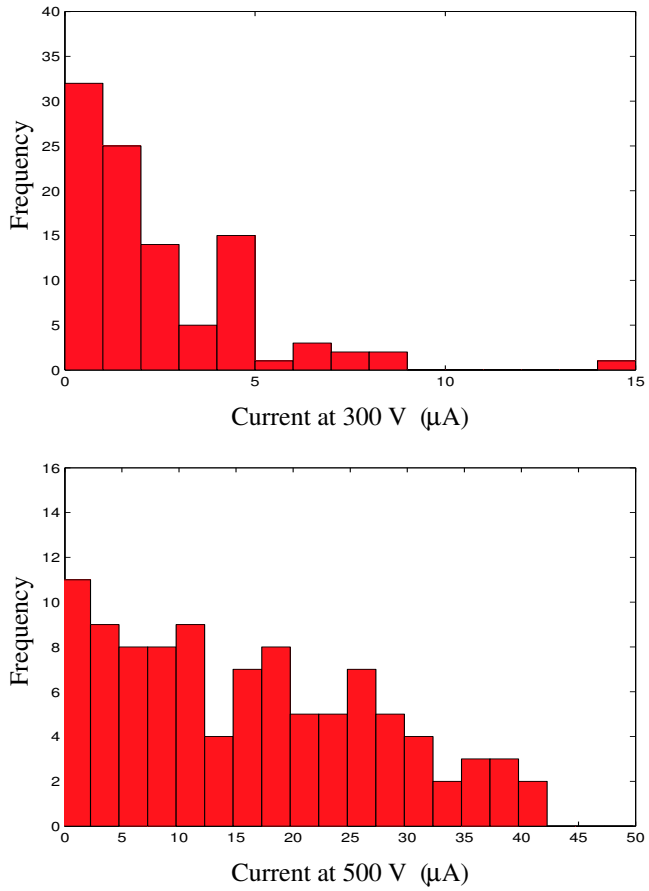

Figure 3: Distribution of the leakage currents measured at 300 V (top) and at 500 V (bottom).

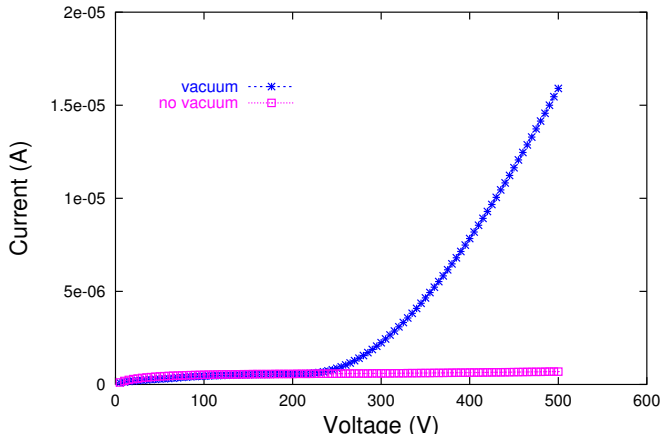

Figure 4: Leakage currents measured with and without vacuum on the chuck of the probe station, for sensor CMS-OB2 number 30210421738319. There is a huge difference between both measurements, not only in the magnitude of the currents but also in the appearance of breakdown when the chuck vacuum is on.

dependence, the leakage currents of about 30 sensors that had shown high currents, were re-measured without chuck vacuum. Huge differences between the currents obtained with and without chuck vacuum were observed. An example of this can be seen in Figure 4, where the current at 500 V decreased by two orders of magnitude when the vacuum was switched off. This is due to the mechanical strain that the chuck vacuum produces on the sensors. It is quite likely that local defects in the silicon are generating excess currents while under strain, since the sensors are naturally warped by ~ 60 μm. It can also be seen that the sensor did not evidence breakdown up to 500 V when the chuck vacuum was switched off, whilst before this sensor showed a clear breakdown at ~ 250 V. This behaviour is representative of what was observed on the other sensors. The STM sensors showed a large sensitivity to any kind of mechanical tension.

For comparison, the same test was done for other prototype sensors manufactured by HPK, one GLAST2000 sensor and one LHCb Multi-Geometry sensor, since we have not yet received CMS-OB2 sensors from this company. A description of these sensors and their characteristics can be found in [3, 8, 9]. In Figure 5, the currents with and without chuck vacuum measured for these sensors are shown. It can be seen that the currents do not depend on the application of vacuum to the chuck of the probe station for any of

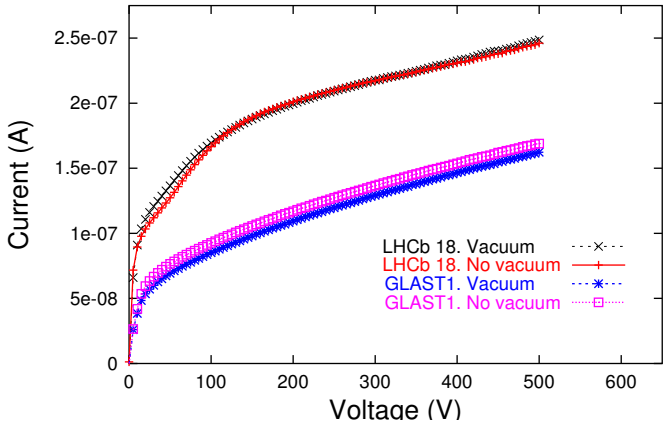

Figure 5: Leakage currents measured with and without chuck vacuum, for two different sensors, one GLAST sensor and one LHCb sensor. The currents do not depend on the application of vacuum to the chuck.

those sensors, as it was the case for the CMS-OB2 sensors from STM.

A comparison was made between the currents that we measured and the data provided by CMS. Even without vacuum, we found the currents to be higher than the numbers quoted by CMS, since they found all currents to be quite small, below 2 μA at 500 V, whilst we reach up to 20 μA at the same voltage.

The dependence of the currents on the relative humidity (RH) was also investigated. Whilst the humidity was changed, two series of measurements were performed, with and without vacuum on the chuck. Figure 6 shows that the currents were found to depend only slightly on the relative humidity. The humidity is definitively not the most important factor affecting the currents.

Correlations between high currents and bad visual inspection grading were also investigated, but no conclusive results were obtained.

From the IV curves, the breakdown voltages can be extracted. We define the breakdown voltage as the reverse bias voltage at which a sharp increase in the current occurs. Above breakdown, the reverse current increases very rapidly with a slight increase in the reverse voltage. In Figure 7, a distribution of the observed breakdown voltages with chuck vacuum is shown. A breakdown voltage $V_{break} = 0$ was assigned to the sensors that do not evidence breakdown below 500 V. It can be seen that most of the sensors have breakdown between 200 V and 350 V, or they do not exhibit a breakdown up to voltages of 500 V. Without chuck vacuum, most of the sensors do not

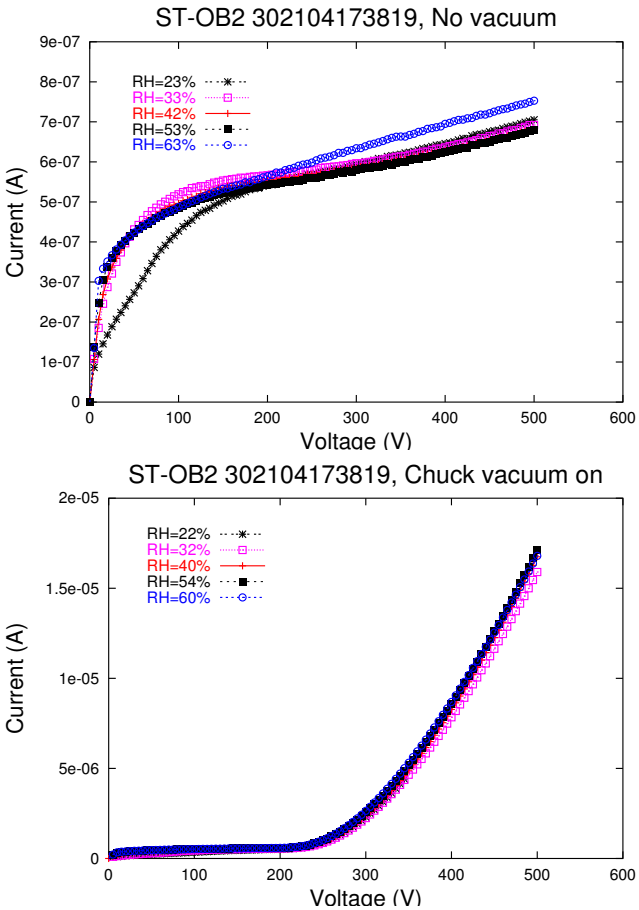

Figure 6: Leakage currents measured at different RH, without vacuum on the chuck (top), and with vacuum on the chuck (bottom). The currents depend only slightly on the RH.

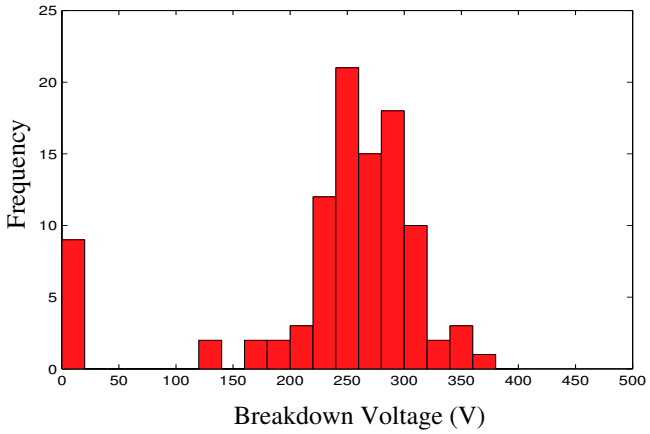

Figure 7: Distribution of the measured breakdown voltages. Breakdown voltage $V_{break} = 0$ is assigned to the sensors that do not evidence breakdown below 500 V.

evidence breakdown below 500 V.

The repeatability of the IV curves under stable conditions (same strain, temperature and relative humidity) was checked for $\sim$ 10% of the sensors. About 30 IV curves on each sensor were taken, waiting 35 min between measurements. In Figure 8, an example of this test is shown, where it can be seen how the curves are consistent within $\pm$5%. The curves were found to be reproducible in this test. Note that the sensors were not moved from the chuck between measurements, and only the voltage was ramped up and down.

Moreover, the current stability of 10% of the sensors was investigated and verified in a $\sim$ 30 h long biasing test, while temperature and humidity were monitored. No significant variations of the leakage current were observed over the duration of this test, as can be seen in Figure 9.

Overall, the leakage currents were stable and reproducible against long term drifts as long as the vacuum on the chuck was kept constant.

2.3 Depletion Voltage

The bulk capacitance of the sensor is the capacitance of all readout strips to the backplane. It is proportional to the inverse of the square root of the bias voltage applied to the sensor until full depletion is reached, and then assumes a constant value. The bulk capacitance was measured as a function of the biasing voltage in order to determine the full depletion voltage. This can

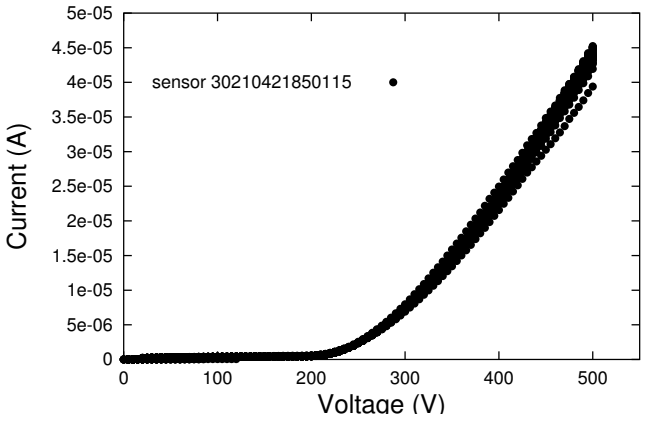

Figure 8: Leakage currents taken for one sensor as a test of repeatability. The 30 IV-curves shown in the plot were taken during night, waiting 35 minutes between them.

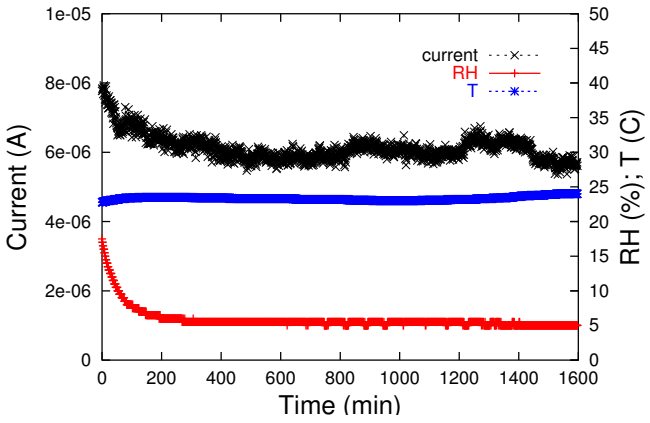

Figure 9: Current stability test for sensor 30210421741713. The sensor was biased at 450 V during 27 hours. The relative humidity and temperature are plotted to see the evolution of the ambient conditions. No significant variations of the leakage current were observed.

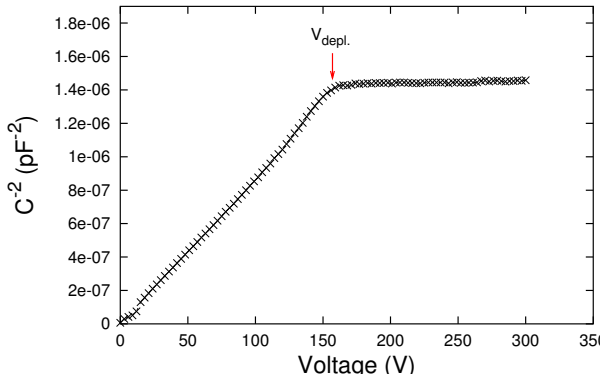

Figure 10: The full depletion voltage is extracted from the $1/C^2$ as a function of the bias voltage curves as the intersection of two straight lines. Shown is a typical curve, corresponding to sensor 30210414739808. The depletion voltage is indicated by the arrow.

be determined as the bias voltage at which the detector capacitance reaches a constant value. We plot $1/C^2$ as a function of the bias voltage and we estimate the depletion voltage as the intersection of two straight lines fitted to the rising part and the flat part of the curve, respectively. The depletion voltage determines the operation voltage of the sensors. It is, therefore, a very important information for module assembly, since sensors should be matched in depletion voltage when they are mounted on the same ladder.

The capacitance measurements were performed on all sensors by connecting a Keithley 487 unit working as a voltage source, and a HP 4192 LCR meter between the bias line and the backplane. The CV curves were made using a measuring frequency of 1 kHz and a signal amplitude of 1 V. Figure 10 shows a typical curve of $1/C^2$ as a function of the bias voltage.

Figure 11 shows the distribution of the obtained full-depletion voltages. All of them are between 140 and 280 V. According to CMS specifications, sensors should fully deplete between 100 and 300 V, which is fulfilled by all of them.

A comparison between the full depletion voltages that we measured and the data provided by CMS is shown in Figure 12. A clear correlation between both data sets is observed, although we have a trend in assigning slightly higher depletion voltages.

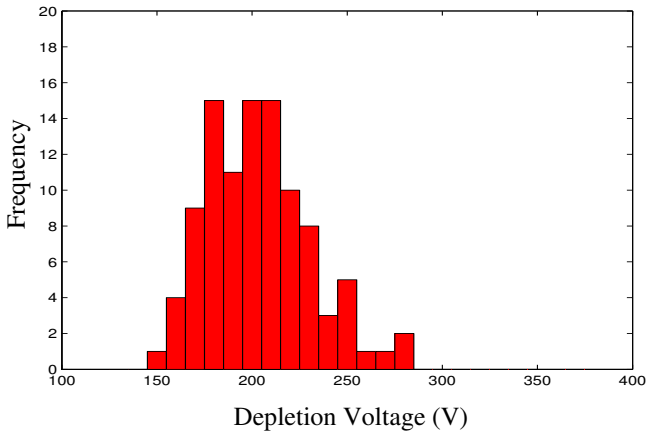

Figure 11: Distribution of the measured depletion voltages. All the sensors deplete between 140 and 280 V, fulfilling the specifications.

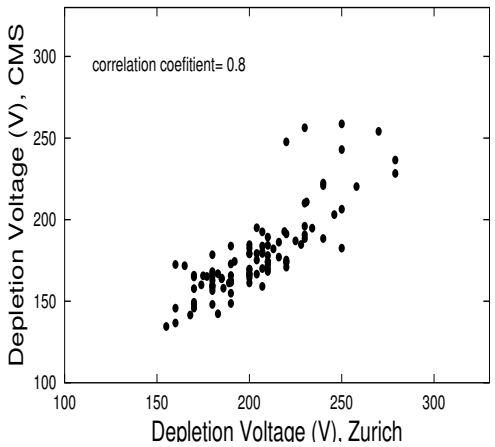

Figure 12: Comparison between the depletion voltages measured by CMS and our measurements. The values are clearly correlated.

2.4 Tests with automatic probe station

The coupling capacitance is the capacitance between the strip implant and the read-out aluminium line. Its measurement allows to detect certain classes of bad strips, which are characterized by a metal open, a metal short or a pinhole in the dielectric substrate of the coupling capacitor.

Coupling capacitance measurements were performed using an Electroglas 1034XA6 automatic probe station, a probe card for contacting AC- and DC-pads on the sensor, and a HP 4192A LCR meter. The probe station and the LCR meter were controlled via GPIB bus by Labview programs running on a PC. The measurements were performed by contacting the AC- and DC- pads of one strip simultaneously with the probe card, in order to determine the coupling capacitances of the strip with the LCR meter. The measurements were taken at a frequency of 1 kHz and a signal amplitude of 1 V [10].

The measurements were carried out on about 15% of the sensors, which were selected as containing bad strips according to the list provided by CMS. Pinholes and anomalous capacitance values were detected on the sensors. The bad channels observed in our coupling capacitor scans were compared to the list provided by CMS. From the total of 8704 inspected strips, 35 strips were flagged as bad by CMS as containing pinholes and having capacitance values out of specification. From them, we could clearly detect 32, and for the remaining three we saw evidences. We could not verify, however, 11 strips flagged as bad capacitance without pinhole by CMS, and 12 strips flagged as pinholes without bad capacitance. We found two additional bad strips. These strips are listed in Table 4.

An example of the obtained coupling capacitance profiles is shown in Figure 13. Three strips have coupling capacitors out of specification due to pinholes in the oxide. The number of defective strips per sensor is specified to be less than 1%. All inspected sensors were below this number.

In the future, we plan to do this test only on sensors that show suspicious features during visual inspection and that have bad strips as flagged by the vendor.

2.5 Metrology

Metrological measurements were performed in order to determine the warp of the sensors and to verify the cutting line precision and parallelity, as well as other geometrical features on the sensors. The parallelity and precision of the cut edges are important due to the proposed ladder assembly procedure [11], which exploits the accuracy of the dicing edge of the sensors for alignment purposes. In an assembly template, the sensors are pushed with their cut

Table 4: List of strips flagged as containing pinholes or capacitor values out of specification by CMS, and strips flagged as bad in our set up.

Sensor ID	Bad strips (CMS)		Bad strips (Zürich)
	Pinholes	Bad Capacitor	
30210421628615	491, 490, 489	491, 490, 489	491, 490, 489
30210423863701	281, 346, 348, 350	281, 346, 348, 70	281, 346, 348
30210431215506	509, 189, 168	509, 189	509, 189
30210422067707	500, 217, 48, 18	500, 6, 48, 18	500, 48, 18
30210421741420	488, 465, 464, 458	488, 465, 464, 458	488, 465, 464, 458
30210421958406	426, 277, 274, 113	426, 277, 274, 113	426, 277, 274, 113
30210421849011	432, 326, 182	432, 244, 182	432, 182
30210421741411	103, 99, 96, 88	-	-
30210414739808	263, 243, 29	263, 243, 29	263, 243, 29
30210431403515	60, 56, 48, 35	60, 56, 48, 35, 4	60, 56, 48, 35
30210421850216	144, 103, 104, 105, 106	144	144, 357
30210422302601	75, 76	75, 76	75, 76
30210423863717	450	450, 385, 187, 186, 70	450, 187, 186
30210424086721	-	454, 304, 165, 164, 70	165, 164, 383
30210423860507	346, 172	474, 346, 172	346, 172
30210421741619	505, 68	68, 41	505, 68
30210431300203	-	455, 311, 310, 309, 308	311, 310, 309, 308

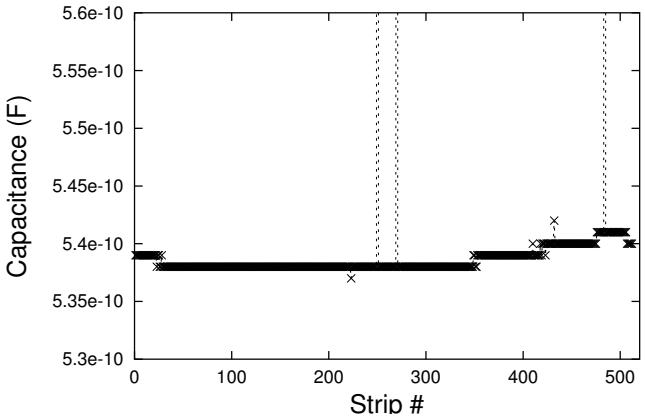

Figure 13: Coupling capacitance as a function of the strip number for sensor 30210414739808. Strips 250, 270 and 484 have coupling capacitors out of specifications, with values of up to 2 mF that are out of the scale of this plot. The profile of the coupling capacitors across the sensor is likely to be related to process inhomogeneities.

edges against posts in order to align the sensors with respect to each other and with respect to alignment pins in the ladder support.

According to specifications, the flatness should be such that the wafer warp is less than 100 μm, and the dicing accuracy should be better than 20 μm [4].

About 70 sensors were characterised on an optical metrology machine[1] in order to verify the mechanical specifications. Several parameters were measured, although the metrology grading procedure was based only on some of them: flatness, overall length and width of the sensor, distance between the edge and the strips, and parallelity between the edge and the strips. Four out of 70 sensors were classified as B grade, whilst the remaining were classified as A grade. The B grade sensors were found to present anomalies on the width or length, and also non-parallelity between the edge and the strips.

Figure 14 shows the distribution of the measured overall width and length for the sensors. There are three sensors that have values far from the mean value, and were therefore considered as B grade sensors. The mean values of the sensor outer dimensions are within 6 μm of the nominal values. Moreover, the standard deviation from sensor to sensor is better than 5 μm.

[1]Mahr OMS 600.

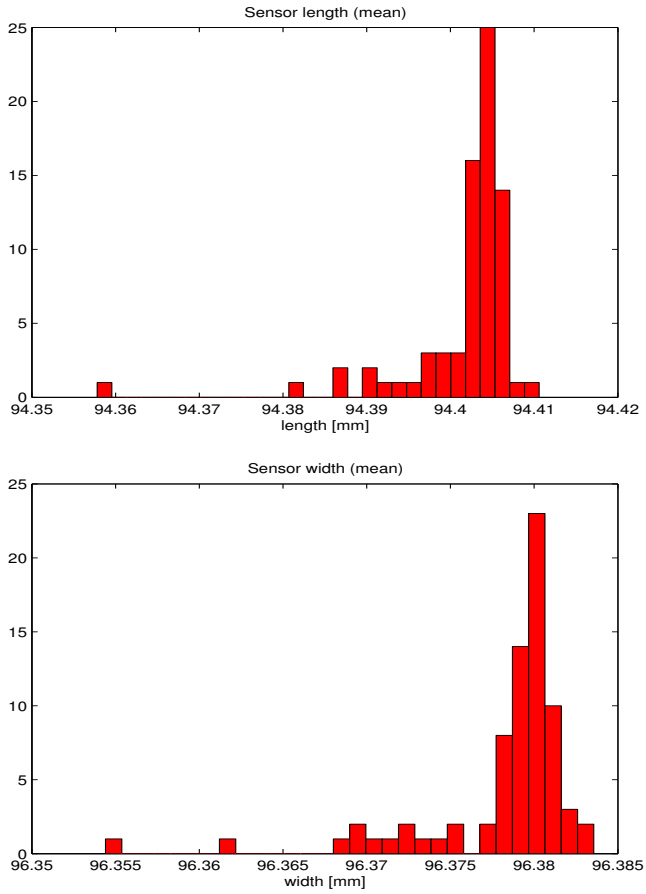

Figure 14: Distribution of the measured overall length (top) and width (bottom) for 70 sensors. The mean length is 94.402 mm, and the mean width is 96.378 mm.

Figure 15 shows the distribution of the measured parallelities between the sensor edge and the closest strip, for both sides of the sensor. For each sensor, the coordinates of ten points belonging to the edge were measured. By fitting them to a straight line, the edge was reconstructed. The same procedure was repeated for the closest strip. The assigned paralletity is $L \tan\theta$, L being the sensor edge length and θ the angle between the reconstructed lines. The mean parallelity accuracy was determined to be ~ 5 μm. Some anomalous values can clearly be seen in the histogram, and these sensors were classified as B grade sensors. There are two sensors with anomalous width and length having as well anomalous parallelity. The other two sensors classified as B grade, failed in a single feature.

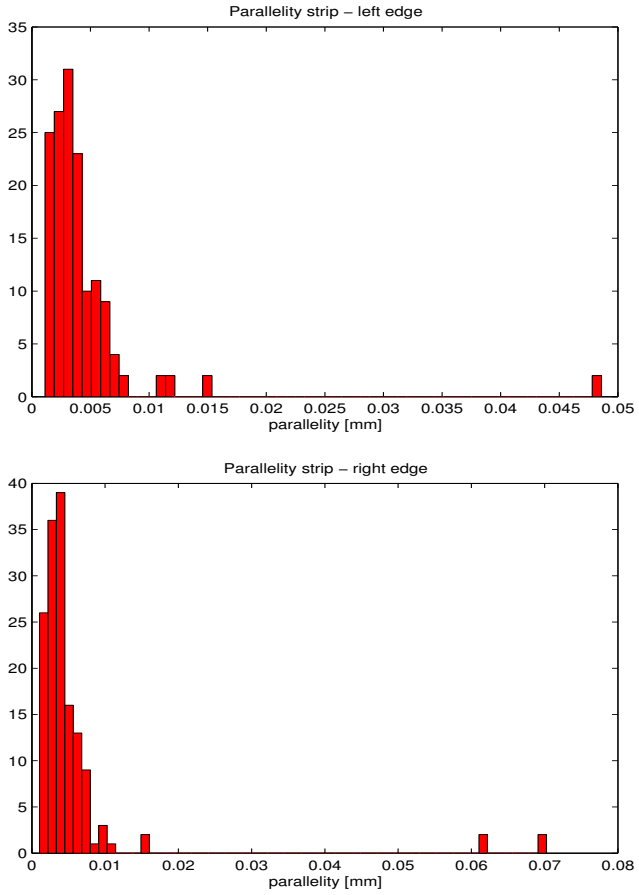

Figure 15: Distribution of the measured parallelities between the sensor edge and the closest strip, for both sides of the sensors.

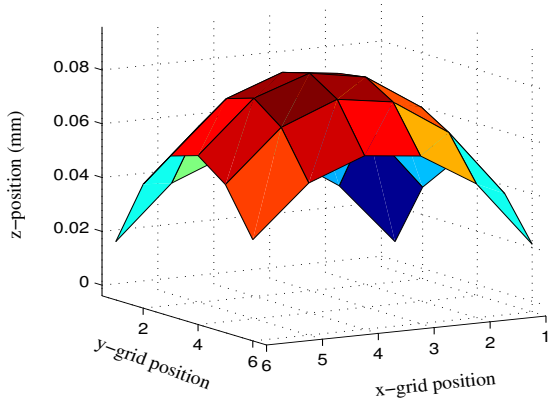

Figure 16: The z-profile of a sensor is shown. The measured points are connected by surface grid lines. The z-coordinates were recorded on an equidistant grid of 6×6 points covering the full surface of the sensor.

The flatness of the sensors was determined by measuring a profile of the surface height of the sensor laying freely on a flat surface, with the strip side facing upwards. On each sensor, z-coordinates have been recorded on an equidistant grid of 6×6 points covering the full surface of the sensor. A typical example of the obtained profiles is shown in Figure 16. It shows a characteristic sensor deflection of 60 μm over the full length of 94 mm and width of 96 mm. The distribution of the measured warp for all inspected sensors is shown in Figure 17. The mean warp was determined to be ~ 60 μm, and the maximum measured warp was ~ 100 μm, fulfilling specifications.

2.6 Overall sensor grading

Depending on the results of the tests described above, an overall grading is assigned to each sensor. The sensors are classified according to the following criteria:

- Grade-A: good sensors, graded as A in the visual inspection, and leakage currents $I < 20$ μA at 500 V, and less than two bad strips per sensor, and graded as A in the metrology tests.
- Grade-B: medium sensors, graded as B in the visual inspection, or

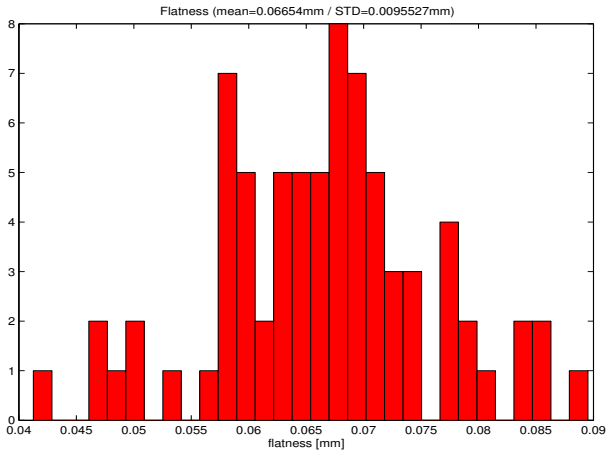

Figure 17: Distribution of the measured flatness on the sensors.

leakage currents $20 < I < 30$ μA at 500 V, or between 2 and 6 bad strips per sensor, and graded as A in the metrology tests.

- Grade-C: poor sensors, graded as C or D in the visual inspection, or leakage currents $I > 30$ μA at 500 V, or more than 6 bad strips per sensor, or graded as B in the metrology tests.
- Grade-X: destroyed.

Grade-A sensors should be used in the inner parts of the detector, whilst grade-B sensors could be used for the rest or as spare. Grade-C sensors should not be used, neither as detector nor as spare. In the overall grading, 20% of the sensors were classified as grade-A sensors, 54% were classified as grade-B, and 25% were classified as grade-C. One sensor was destroyed during the tests.

3 Database and web page

All information from sensor probing of the 100 ST OB2 sensors is stored in a mySQL-based [12] database. A web based query is used, with an interface to PHP [13] (a web oriented scripted language to query from html). It allows to store, query, and retrieve vendor and testing information on the sensors, and is used to track or select components during module construction. A screen-shot of the graphical user interface is shown in Figure 18. Shown is a summary of measurements and gradings, together with comments for some of the sensors. Further details can be found in [14].

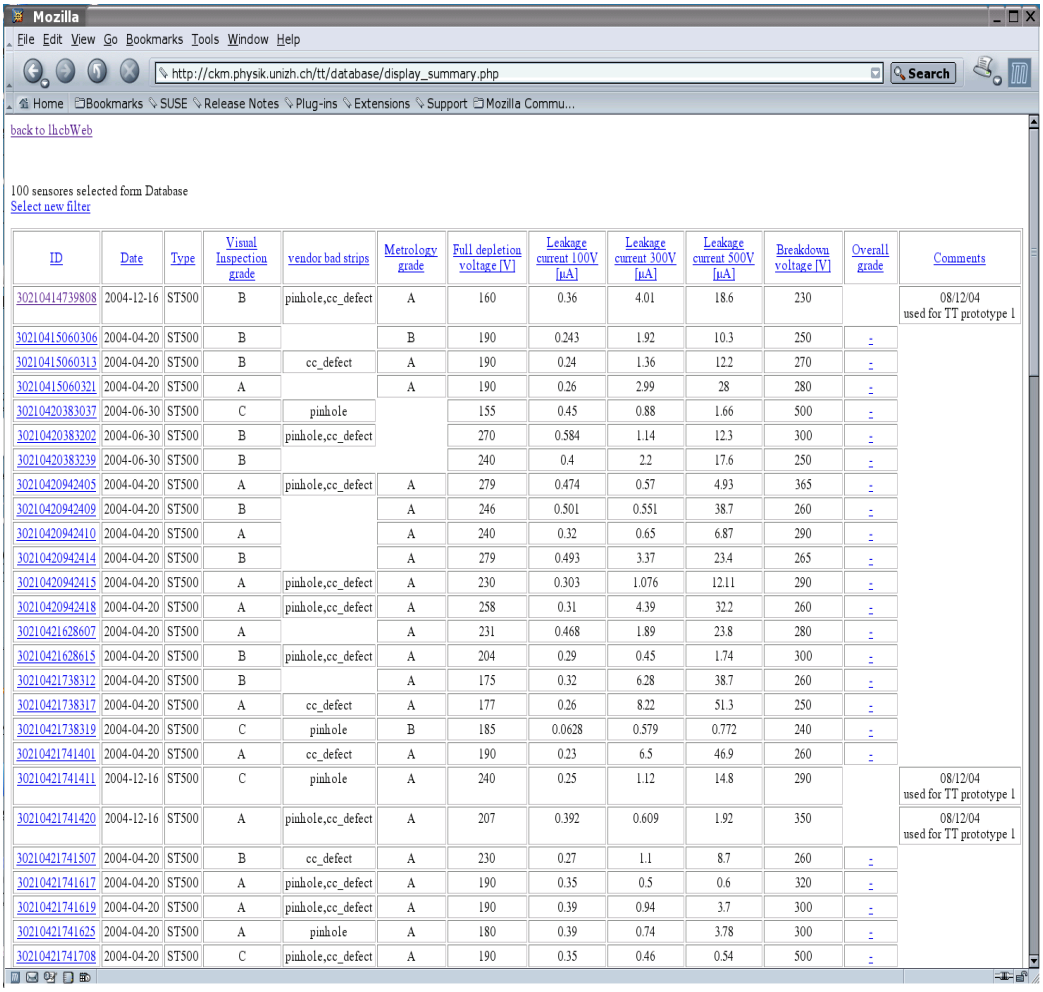

ID	Date	Type	Visual Inspection grade	vendor bad strips	Metrology grade	Full depletion voltage [V]	Leakage current 100V [µA]	Leakage current 300V [µA]	Leakage current 500V [µA]	Breakdown voltage [V]	Overall grade	Comments
30210414739808	2004-12-16	ST500	B	pinhole,cc_defect	A	160	0.36	4.01	18.6	230		08/12/04 used for TT prototype 1
30210415060306	2004-04-20	ST500	B		B	190	0.243	1.92	10.3	250	-	
30210415060313	2004-04-20	ST500	B	cc_defect	A	190	0.24	1.36	12.2	270	-	
30210415060321	2004-04-20	ST500	A		A	190	0.26	2.99	28	280	-	
30210420383037	2004-06-30	ST500	C	pinhole		155	0.45	0.88	1.66	500	-	
30210420383202	2004-06-30	ST500	B	pinhole,cc_defect		270	0.584	1.14	12.3	300	-	
30210420383239	2004-06-30	ST500	B			240	0.4	2.2	17.6	250	-	
30210420942405	2004-04-20	ST500	A	pinhole,cc_defect	A	279	0.474	0.57	4.93	365	-	
30210420942409	2004-04-20	ST500	B		A	246	0.501	0.551	38.7	260	-	
30210420942410	2004-04-20	ST500	A		A	240	0.32	0.65	6.87	290	-	
30210420942414	2004-04-20	ST500	B		A	279	0.493	3.37	23.4	265	-	
30210420942415	2004-04-20	ST500	A	pinhole,cc_defect	A	230	0.303	1.076	12.11	290	-	
30210420942418	2004-04-20	ST500	A	pinhole,cc_defect	A	258	0.31	4.39	32.2	260	-	
30210421628607	2004-04-20	ST500	A		A	231	0.468	1.89	23.8	280	-	
30210421628615	2004-04-20	ST500	B	pinhole,cc_defect	A	204	0.29	0.45	1.74	300	-	
30210421738312	2004-04-20	ST500	B		A	175	0.32	6.28	38.7	260	-	
30210421738317	2004-04-20	ST500	A	cc_defect	A	177	0.26	8.22	51.3	250	-	
30210421738319	2004-04-20	ST500	C	pinhole	B	185	0.0628	0.579	0.772	240	-	
30210421741401	2004-04-20	ST500	A	cc_defect	A	190	0.23	6.5	46.9	260	-	
30210421741411	2004-12-16	ST500	C	pinhole	A	240	0.25	1.12	14.8	290		08/12/04 used for TT prototype 1
30210421741420	2004-12-16	ST500	A	pinhole,cc_defect	A	207	0.392	0.609	1.92	350		08/12/04 used for TT prototype 1
30210421741507	2004-04-20	ST500	B	cc_defect	A	230	0.27	1.1	8.7	260	-	
30210421741617	2004-04-20	ST500	A	pinhole,cc_defect	A	190	0.35	0.5	0.6	320	-	
30210421741619	2004-04-20	ST500	A	pinhole,cc_defect	A	190	0.39	0.94	3.7	300	-	
30210421741625	2004-04-20	ST500	A	pinhole	A	180	0.39	0.74	3.78	300	-	
30210421741708	2004-04-20	ST500	C	pinhole,cc_defect	A	190	0.35	0.46	0.54	500	-	

Figure 18: Screen-shot of the graphical user interface.

4 Conclusions

We have presented the sensor quality assurance program that will be followed by the LHCb Silicon Tracker group. We have performed quality control tests on the first pre-production 100 CMS-OB2 sensors, produced by STM. Our main results are the following:

- Visual inspection over the 100 sensors was performed in order to detect macroscopic defects like scratches, chipped edges, pad contamination, as well as the sensor cleanliness. Only 49% of the sensors were found to be free of defects, although 84% could be used in a detector ladder.

- Leakage current measurements were performed on all 100 sensors. They were found to be very different from sensor to sensor, and only 60% fulfill specifications if chuck vacuum is applied. High currents could be reduced greatly when the sensors were not held by vacuum, and therefore we relate this effect to the presence of mechanical strain, which might enlarge local defects in the sensors. No significant variations of the currents with relative humidity were found. Currents were repeatable and stable over time of operation, as was verified on a sample of 15% of the sensor that were chosen randomly.

- Depletion voltages were measured for all 100 sensors. All sensors fulfill specifications, showing depletion voltages in the range of 140-280 V.

- Coupling capacitance measurements were performed on 15% of the sensors using an automatic probe station. From the total of 8704 inspected strips, 35 strips were flagged as bad by CMS, containing pinholes and bad capacitances. From them, we could clearly detect 32, and for the remaining three we saw evidences. We could not verify, however, 11 strips flagged as bad capacitance only by CMS, and 12 strips flagged as pinholes only. We found two additional bad strips. The number of strip defects per sensor is below 1% on all sensors, satisfying specifications.

- Metrological measurements were performed on 70% of the sensors in order to verify the cutting line precision and parallelity and determine the warp of the sensors, as well as other geometrical features. The mean warp of the sensors was determined to be ~ 60 μm, and the mean parallelity ~ 5 μm. The mean values of the sensor outer dimensions are within 6 μm of the nominal values. Moreover, the standard deviation from sensor to sensor is better than 5 μm.

- According to the overall grading, 20% of the sensors were classified as A grade sensors, 54% were classified as B grade, and 25% were classified as C grade sensors.

From these results, the guidelines and procedures for sensor probing that will be followed by the LHCb Silicon Tracker were established.

References

[1] LHCb collaboration. *LHCb Technical Design Report, Reoptimized Detector Design and Performance.* CERN/LHCC 2003-030.

[2] J. Gassner, M. Needham, and O. Steinkamp. *Layout and Expected Performance of the LHCb TT Station.* LHCb note 2003-140.

[3] J. Gassner, St. Heule, F. Lehner, and C. Lois. *Capacitance measurements on silicon micro-strip detectors for the TT station of the LHCb experiment.* LHCb note 2003-081.

[4] J.-L. Agram *et al.* *The Silicon Sensors for the Compact Muon Solenoid Tracker - Design and Qualification Procedure* (2003). CMS note 2003/015.

[5] CMS Tracker Sensor Working Group. *Specifications for the Quality Control & Assurance of the CMS Silicon Sensors* (2000).

[6] *Supply of Silicon Micro-strip Sensors for the CMS Silicon Strip Tracker (SST)* (2000). Invitation to Tender: IT-2777/EP/CMS. Technical Specification.

[7] A. Cattai. *Large-scale module production for the CMS silicon strip tracker.* Presented at Int. Symp. on the Development and Application of Semiconductor Tracking Detectors, Hiroshima, Japan, June 14-17, 2004. To be published in Nucl. Instr. and Meth. A.

[8] F. Lehner, P. Sievers, O. Steinkamp, U. Straumann, and M. Ziegler. *Description and Characterization of Inner Tracker Silicon Prototype Sensors.* LHCb note 2001-036.

[9] N. Virmani, H. Sadrozinski, and T. Ohsugi. *GLAST LAT Silicon Strip Detector (SSD) Quality and Reliability Assurance.* GLAST LAT-CR-00082-03.

[10] F. Lehner, P. Sievers, O. Steinkamp, U. Straumann, A. Vollhardt, and M. Ziegler. *Description and Evaluation of Multi-Geometry Silicon Prototype Sensors for the LHCb Inner Tracker.* LHCb note 2002-038.

[11] J. Gassner, F. Lehner, and S. Steiner. *The production, Testing and Assembly of the LHCb Silicon Trigger Tracker.* LHCb note 2004-109.

[12] `http://www.mysql.com`.

[13] `http://www.php.net`.

[14] `http://ckm.physik.unizh.ch/tt/`.